# Free edge coupling effect of piezoelectric cross-ply laminated plates

**Chao Han[1,*], Zhangjian Wu[1]**

[1] Department of MACE, The University of Manchester, M13 9PL, UK
* Corresponding author: Chao.Han-2@postgrad.manchester.ac.uk

**Abstract**

Free edge effect of laminated plates has been extensively investigated in the past two decades. Due to the boundary condition limitation, very limited work on piezoelectric laminated plates with free edges was carried out. In this paper, coupled and uncoupled analytical analyses on the interlaminar stresses in the vicinity of the free edges of piezoelectric laminated plates are presented on the basis of three-dimensional elasticity and piezoelectricity. The state space equations for cross-ply piezoelectric laminates subjected to uniaxial extension are obtained by considering all independent elastic and piezoelectric constants. The equations satisfy the boundary conditions at free edges and the continuity conditions across the interfaces between plies of the laminates. Three dimensional exact solution is sought and validated by comparing present numerical results with those of existing approximate analytical and finite element models. The singularity of the interlaminar stresses near the free edges is confirmed and the electromechanical coupling effects give much higher interlaminar stresses at the free edges in comparison with those of the corresponding uncoupled cases.

**Keywords:** piezoelectricity, laminated plate, coupling effect, interface stress, exact solution

## 1. Introduction

In recent decades, composite materials have extensive popularity in high-performance products that demand for high-strength, lightweight among many fields. Due to the development of multifunctional structures, smart materials and structures, which can perform sensing, controlling, actuating with distinct direct and converse piezoelectric effects, are widely used in many applications such as structural vibration control, precision positioning, aerospace and nanotechnology. Piezoelectric structures are often made from multi-layered thin films of dissimilar materials in the forms of stacks. For example, a piezoelectric laminated plate with simply-supported conditions, as a multilayer stack, was investigated by many researchers such as Heyliger [1], Lee and Jiang [2], Cheng et al. [3] and Xu et al. [4]. Sheng et al. [5] presented state space solution for laminated piezoelectric plate with clamped and electric open-circuited boundary conditions.

It is well-established that due to the discontinuity of material properties at the interfaces, a highly concentrated interlaminar stress field can occur in the vicinity of the free edges which will lead to interlaminar failures such as delamination or matrix cracking. Pipes and Pagano [6] presented a 3D elastic solution for the free-edge effect for a symmetric laminate strip under uniaxial tension. By using Lekhnitskii's [7] stress potential as well as the eigenfunction technique, Wang and Choi [8] investigated the stress singularities at the free edge of laminated plate. Becker [9] presented a closed-form solution by introducing a particular warp deformation which decays rapidly towards the laminate interior to reflect the free edge effect. Most recently, analytical solutions were developed by Tahani and Nosier [10] within Reddy's layerwise theory (LWT) to investigate the free edge effect problem of general cross-ply laminates with finite dimensions under uniform axial extension. Recently Zhang et al. [11] give the 3D analytical solution for the free edge cracking effect in composite laminates under extension and thermal loading by using state space method.

Due to the piezoelectric coupling effects in piezoelectric laminated plate, the mechanical and electrical behavior becomes more complex. Thus an accurate determination of coupling effect on free edge interlaminar stresses and deformation is essential in the design of elastic and piezoelectric structure. By using Fourier transforms to reduce electro-elastic boundary value problem to the solutions of integral equations, Ye and He [12] solved the problem of electric field concentrations of a pair of parallel electrodes arrayed in one plane. Finite element method was chosen to show the effect of piezoelectric coupling on interlaminar stresses and electric field strengths near the free edge by Artel and Becker [13]. In addition, an analytical solution was also developed to determine the state variables of piezoelectric elasticity in the vicinity of free edges using a layerwise displacement theory by Mirzababaee and Tahani [14].

In this paper, on the basis of 3D elasticity and piezoelectricity, an exact analytical solution that satisfies both mechanical and electric boundary conditions is established by considering continuity of displacements, transverse stresses, electric potentials and vertical electric displacements across interfaces between different materials.

## 2. Fundamental State Space Method Formulation

### 2.1. State space equations for cross-ply piezoelectric plate

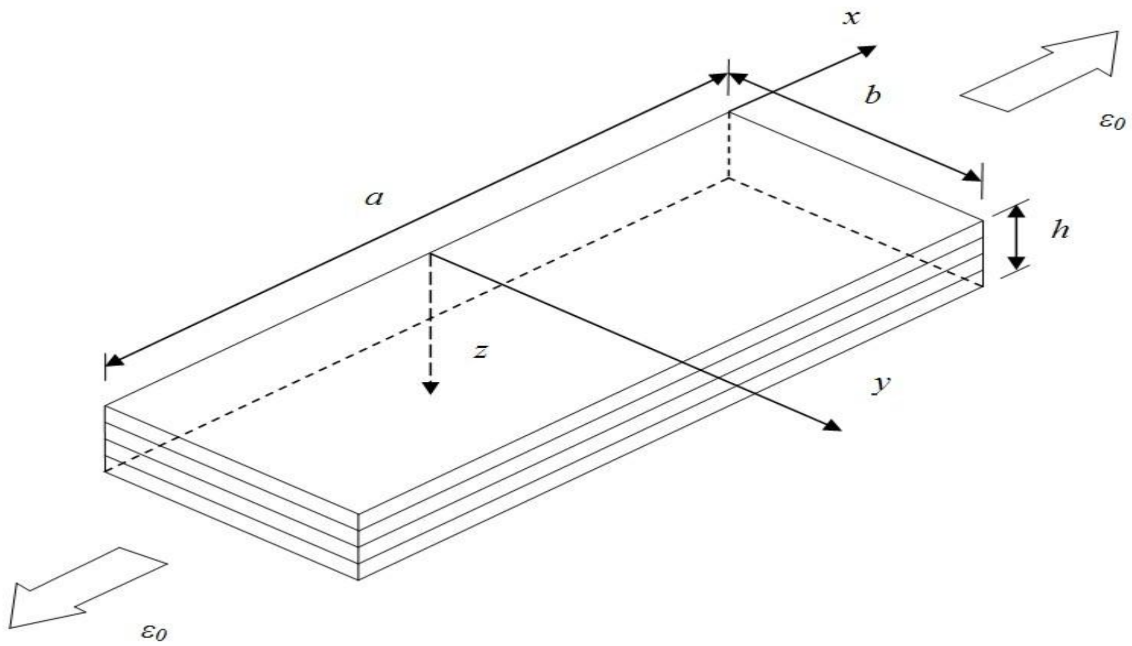


Figure 1. Geometry of a piezoelectric laminated plate

The rectangular piezoelectric laminated plate is subjected to a uniform constant axial strain $\varepsilon_0$ and it is assumed to have length *a*, width *b*, and uniform thickness *h* (Fig. 1). The principle elastic directions of plate coincide with the axes of the chosen rectangular coordinate system and full coupled three-dimensional piezoelectric-elastic constitutive relations of orthotropic piezoelectric lamina are given

$$\{\sigma\} = [C]\{\varepsilon\} - [e]^T \{E\}, \quad (1)$$

$$\{D\} = [e]\{\varepsilon\} + [\in]\{E\}, \quad (2)$$

Where {σ}, {ε}, {*E*} and {*D*} are, respectively, stress, strain, electric field, and electric displacement vectors. [*C*], [*e*] and [ϵ] are elastic, piezoelectric and electric permittivity constants, respectively. Explicit forms of Eqs. (1) and (2) are given as follows:

$$\begin{Bmatrix} \sigma_x \\ \sigma_y \\ \sigma_z \\ \tau_{yz} \\ \tau_{xz} \\ \tau_{xy} \end{Bmatrix} = \begin{bmatrix} C_{11} & C_{12} & C_{13} & 0 & 0 & 0 \\ C_{12} & C_{22} & C_{23} & 0 & 0 & 0 \\ C_{13} & C_{23} & C_{33} & 0 & 0 & 0 \\ 0 & 0 & 0 & C_{44} & 0 & 0 \\ 0 & 0 & 0 & 0 & C_{55} & 0 \\ 0 & 0 & 0 & 0 & 0 & C_{66} \end{bmatrix} \begin{Bmatrix} \varepsilon_x \\ \varepsilon_y \\ \varepsilon_z \\ \gamma_{yz} \\ \gamma_{xz} \\ \gamma_{xy} \end{Bmatrix} - \begin{bmatrix} 0 & 0 & e_{31} \\ 0 & 0 & e_{32} \\ 0 & 0 & e_{33} \\ 0 & e_{24} & 0 \\ e_{15} & 0 & 0 \\ 0 & 0 & 0 \end{bmatrix} \begin{Bmatrix} E_x \\ E_y \\ E_z \end{Bmatrix}, \tag{3}$$

$$\begin{Bmatrix} D_x \\ D_y \\ D_z \end{Bmatrix} = \begin{bmatrix} 0 & 0 & 0 & 0 & e_{15} & 0 \\ 0 & 0 & 0 & e_{24} & 0 & 0 \\ e_{31} & e_{32} & e_{33} & 0 & 0 & 0 \end{bmatrix} \begin{Bmatrix} \varepsilon_x \\ \varepsilon_y \\ \varepsilon_z \\ \gamma_{yz} \\ \gamma_{xz} \\ \gamma_{xy} \end{Bmatrix} + \begin{bmatrix} \epsilon_{11} & 0 & 0 \\ 0 & \epsilon_{22} & 0 \\ 0 & 0 & \epsilon_{33} \end{bmatrix} \begin{Bmatrix} E_x \\ E_y \\ E_z \end{Bmatrix}. \tag{4}$$

Due to the uniform extension $\varepsilon_0$ and infinite length in the $x$ direction, the state variables are independent from the longitudinal coordinate $x$, therefore, the linear strain-displacement relations of elasticity and the components of electric field vector can be written as

$$\begin{aligned} &\varepsilon_x = \frac{\partial u}{\partial x} = \varepsilon_0, \quad \varepsilon_y = \frac{\partial v}{\partial y}, \qquad \varepsilon_z = \frac{\partial w}{\partial z}, \\ &\gamma_{yz} = \frac{\partial w}{\partial y} + \frac{\partial v}{\partial z}, \ \gamma_{xz} = \frac{\partial u}{\partial z} + \frac{\partial w}{\partial x} = 0, \ \gamma_{xy} = \frac{\partial u}{\partial y} + \frac{\partial v}{\partial x} = 0, \\ &E_x = -\frac{\partial \varphi}{\partial x} = 0, \ E_y = -\frac{\partial \varphi}{\partial y}, \qquad E_z = -\frac{\partial \varphi}{\partial z}. \end{aligned} \tag{5}$$

Where $u$, $v$ and $w$ represent displacements in the $x$, $y$ and $z$ directions, respectively.

Gaussian law and stress equilibrium equations of the elastic body are given below

$$\begin{cases} D_{x,x} + D_{y,y} + D_{z,z} - q = 0 \\ \sigma_{x,x} + \tau_{xy,y} + \tau_{xz,z} + f_x = 0 \\ \tau_{xy,x} + \sigma_{y,y} + \tau_{yz,z} + f_y = 0 \\ \tau_{xz,x} + \tau_{yz,y} + \sigma_{z,z} + f_z = 0 \end{cases}. \tag{6}$$

By considering Eqs. (3)-(6) and assuming the electrical body charge $q$ as well as body forces $f_i$ to be zero, we can get $\tau_{xz} = 0$, $\tau_{xy} = 0$, $D_x = 0$ and other 9 state variables $v$, $w$, $\sigma_x$, $\sigma_y$, $\sigma_z$, $\tau_{yz}$, $D_y$, $D_z$, $\varphi$. They are all independent of $x$, and can be expressed as $v(y,z)$, $w(y,z)$, $\sigma_y(y,z)$, $\sigma_z(y,z)$, $\tau_{yz}(y,z)$, $D_y(y,z)$, $D_z(y,z)$, and $\varphi(y,z)$. After a lengthy derivation process based on Eqs. (3)-(6) the following first-order partial differential equations are obtained:

$$\frac{\partial}{\partial z}\{R\} = [A]\{R\} + \{B\}, \tag{7}$$

$$\{R\}=\begin{Bmatrix} v \\ D_z \\ \sigma_z \\ \tau_{yz} \\ \phi \\ w \end{Bmatrix},[A]=\begin{bmatrix} 0 & 0 & 0 & \alpha_{19} & \alpha_{20}\beta & \alpha_{21}\beta \\ 0 & 0 & 0 & -\alpha_{17}\beta & -\alpha_{18}\beta^2 & 0 \\ 0 & 0 & 0 & -\beta & 0 & 0 \\ -\alpha_{13}\beta^2 & -\alpha_{15}\beta & -\alpha_{14}\beta & 0 & 0 & 0 \\ \alpha_5\beta & \alpha_7 & \alpha_6 & 0 & 0 & 0 \\ \alpha_1\beta & \alpha_3 & \alpha_2 & 0 & 0 & 0 \end{bmatrix},\{B\}=\begin{Bmatrix} 0 \\ 0 \\ 0 \\ 0 \\ \alpha_8 \\ \alpha_4 \end{Bmatrix}\varepsilon_0. \quad (8)$$

The following in-plane stresses and electric displacements are also obtained:

$$\begin{Bmatrix} \sigma_x \\ \sigma_y \end{Bmatrix}=\begin{bmatrix} \alpha_9\cdot\beta & \alpha_{10} & \alpha_{11} \\ \alpha_{13}\cdot\beta & \alpha_{14} & \alpha_{15} \end{bmatrix}\begin{Bmatrix} v \\ \sigma_z \\ D_z \end{Bmatrix}+\begin{Bmatrix} \alpha_{12} \\ \alpha_{16} \end{Bmatrix}\varepsilon_0,$$

$$D_y=\begin{bmatrix} \alpha_{17} & \alpha_{18}\cdot\beta \end{bmatrix}\begin{Bmatrix} \tau_{yz} \\ \phi \end{Bmatrix}. \quad (9)$$

Constants related to material property can be expressed as follows:

$$\alpha_1=\frac{-e_{32}\cdot e_{33}-C_{23}\cdot\in_{33}}{\Delta_1},\ \alpha_2=\frac{\in_{33}}{\Delta_1},\ \alpha_3=\frac{e_{33}}{\Delta_1},\ \alpha_4=\frac{-e_{31}\cdot e_{33}-C_{13}\cdot\in_{33}}{\Delta_1},\ \alpha_5=\frac{C_{33}\cdot e_{32}-C_{23}\cdot e_{33}}{\Delta_1},$$

$$\alpha_6=\frac{e_{33}}{\Delta_1},\ \alpha_7=\frac{-C_{33}}{\Delta_1},\ \alpha_8=\frac{C_{33}\cdot e_{31}-C_{13}\cdot e_{33}}{\Delta_1},\ \alpha_9=C_{12}+\alpha_1\cdot C_{13}+\alpha_5\cdot e_{31},\ \alpha_{10}=\alpha_2\cdot C_{13}+\alpha_6\cdot e_{31},$$

$$\alpha_{11}=\alpha_3\cdot C_{13}+\alpha_7\cdot e_{31},\ \alpha_{12}=C_{11}+\alpha_4\cdot C_{13}+\alpha_8\cdot e_{31},\ \alpha_{13}=C_{22}+\alpha_1\cdot C_{23}+\alpha_5\cdot e_{32}, \quad (10)$$

$$\alpha_{14}=\alpha_2\cdot C_{23}+\alpha_6\cdot e_{32},\ \alpha_{15}=\alpha_3\cdot C_{23}+\alpha_7\cdot e_{32},\ \alpha_{16}=C_{12}+\alpha_4\cdot C_{23}+\alpha_8\cdot e_{32},$$

$$\alpha_{17}=\frac{e_{24}}{C_{44}},\ \alpha_{18}=-\frac{e_{24}^2}{C_{44}}-\in_{22},\ \alpha_{19}=\frac{1}{C_{44}},\ \alpha_{20}=-\frac{e_{24}}{C_{44}},\ \alpha_{21}=-1,\ \Delta_1=e_{33}^2+C_{33}\cdot\in_{33},\ \beta=\frac{\partial}{\partial y}.$$

Assuming that the displacements $v$ can be expressed as:

$$v(y,z)=\bar{v}(y,z)+v^{(0)}(z)\cdot(1-\frac{2y}{b}), \quad (11)$$

Where $v^{(0)}(z)$ is the unknown boundary displacement function that can be determined by imposing traction free conditions and open-circuit conditions on the free edges. The following Fourier series expansions are used:

$$\begin{cases} \bar{v}(y,z)=\sum_{n=0}^{\infty}\bar{v}_n(z)\cdot Sin(\eta\cdot y) \\ D_z(y,z)=\sum_{n=0}^{\infty}D_n(z)\cdot Cos(\eta\cdot y), \\ \sigma_z(y,z)=\sum_{n=0}^{\infty}Z_n(z)\cdot Cos(\eta\cdot y) \end{cases} \begin{cases} \tau_{yz}(y,z)=\sum_{n=0}^{\infty}Y_n(z)\cdot Sin(\eta\cdot y) \\ \phi(y,z)=\sum_{n=0}^{\infty}\phi_n(z)\cdot Cos(\eta\cdot y), \\ w(y,z)=\sum_{n=0}^{\infty}w_n(z)\cdot Cos(\eta\cdot y) \end{cases} \quad (12)$$

$$y=-\frac{2b}{\pi}\sum_{n=0}^{\infty}\frac{Cos(n\pi)}{n}\cdot Sin(\eta\cdot y), \quad (13)$$

Where $\eta = n\pi/b$, since a uniformly distributed extension is applied, displacement $v$ is zero at $y = b/2$.

By introducing Eqs. (11)-(13) into Eq. (7) the following non-homogeneous state space equation for an arbitrary value of $n$ is obtained:

$$\frac{d}{dz}\{R_n(z)\} = \left[\overline{A}_n\right]\{R_n(z)\} + \{B_n(z)\}, \tag{14a}$$

Where
$$\{R_n(z)\} = \left[\overline{v}_n(z) \quad D_n(z) \quad Z_n(z) \quad Y_n(z) \quad \phi_n(z) \quad w_n(z)\right]^T, \tag{14b}$$

$$\left[\overline{A}_n\right] = \begin{bmatrix} 0 & 0 & 0 & \alpha_{19} & -\alpha_{20}\eta & -\alpha_{21}\eta \\ 0 & 0 & 0 & -\alpha_{17}\eta & \alpha_{18}\eta^2 & 0 \\ 0 & 0 & 0 & -\eta & 0 & 0 \\ \alpha_{13}\eta^2 & \alpha_{15}\eta & \alpha_{14}\eta & 0 & 0 & 0 \\ \alpha_5\eta & \alpha_7 & \alpha_6 & 0 & 0 & 0 \\ \alpha_1\eta & \alpha_3 & \alpha_2 & 0 & 0 & 0 \end{bmatrix}, \tag{14c}$$

$$\{B_0(z)\} = \begin{Bmatrix} 0 \\ 0 \\ 0 \\ 0 \\ -\frac{2}{b}\cdot\alpha_5\cdot v^{(0)}(z) + \alpha_8\cdot\varepsilon_0 \\ -\frac{2}{b}\cdot\alpha_1\cdot v^{(0)}(z) + \alpha_4\cdot\varepsilon_0 \end{Bmatrix}, \{B_n(z)\} = \begin{Bmatrix} -\frac{2(1+Cos(n\pi))}{n\pi}\cdot\frac{dv^{(0)}(z)}{dz} \\ 0 \\ 0 \\ 0 \\ 0 \\ 0 \end{Bmatrix}. \tag{14d}$$

The solution of non-homogeneous state space equation in Eq. (14) can be obtained as

$$\{R_n(z)\} = e^{\left[\overline{A}_n\right]\cdot z}\{R_n(0)\} + \int_0^z e^{\left[\overline{A}_n\right]\cdot(z-\tau)}\{B_n(\tau)\}d\tau = \left[G_n(z)\right]\{R_n(0)\} + \{H_n(z)\},\ z\in[0,h], \tag{15}$$

Where $[G_n(z)]$ is called transfer matrix and $\{H_n(z)\}$ is non-homogeneous vector.

Consider the piezoelectric laminated plate consists of $N$ different plies and suppose a ply is composed of $K$ fictitious sub-layers. It is assumed that thickness of all the fictitious sub-layers approaches zero uniformly as $K$ is sufficient large. In addition different plies may have different materials, which leads to in-plane stresses discontinuity at the interface. For an arbitrary sub-layer $j$ in $i$th ply, we can establish its state equation:

$$\{R_n(z_i)\}_{i,j} = \left[G_n(z_i)\right]_{i,j}\{R_n(0)\}_{i,j} + \{H_n(z_i)\}_{i,j},\ z_i\in[0,d_i] \tag{16}$$

The non-homogeneous vector $\{H_n(z_i)\}_{i,j}$ from above equation contains unknown boundary functions and their derivatives. As discussed before, we divide $i$th ply into $K_j$ thin sub-layers. The thickness of each sub-layers is $d_i = h_i/k_i$. If the fictitious sub-layer is sufficiently thin, it is reasonable to assume that the unknown functions are linearly distributed within the thin layers in the $z$-direction:

$$\begin{gathered} v_{i,j}^{(0)}(z) = v_{i,j}^t\cdot\left(1-\frac{z}{d_{i,j}}\right) + v_{i,j}^b\cdot\left(\frac{z}{d_{i,j}}\right), \\ z\in[0,d_i], i=1,2,\cdots N, j=1,2,\cdots K_i. \end{gathered} \tag{17}$$

Where $v_{i,j}^t$, $v_{i,j}^b$ are the end values of $v_{i,j}^{(0)}(z)$ at the top and bottom surfaces of the $j$th thin sub-layers, respectively.

By imposing continuity conditions at the interface of adjacent sub-layers $\{R_n(d_i)\}_{i,j} = \{R_n(0)\}_{i,j+1}$ and adjacent plies $\{R_n(h_i)\}_i = \{R_n(0)\}_{i+1}$, we can obtain the relationship between the state variables of the bottom and top surfaces of the plate as follows

$$\{R_n(h_N)\} = [\Pi]\{R_n(0)\} + \{\overline{\Pi}\}, \tag{18}$$

Where $\{R_n(0)\}$ and $\{R_n(h_N)\}$ are the state vectors of top and bottom surfaces of the plate, respectively, and $[\Pi]$ is the state transfer matrix. The non-homogeneous vector $\{\overline{\Pi}\}$ contains $K_1 + K_2 + \cdots + K_N + 1$ boundary unknown coefficients $v_{i,j}^t$ , $v_{i,j}^b$ which can be determined by mechanical and electric boundary conditions at the free and electric open-circuited edges.

### 2.2. Boundary conditions of cross-ply piezoelectric plate

For an electric load free surface, open-circuited and traction-free conditions are considered, the top and bottom surface conditions are obtained:

$$\begin{bmatrix} D_n(0) & Z_n(0) & Y_n(0) & \tau_{xz}(0) \end{bmatrix}^T = \begin{bmatrix} 0 & 0 & 0 & 0 \end{bmatrix}^T, \tag{19a}$$

$$\begin{bmatrix} D_n(h_N) & Z_n(h_N) & Y_n(h_N) & \tau_{xz}(h_N) \end{bmatrix}^T = \begin{bmatrix} 0 & 0 & 0 & 0 \end{bmatrix}^T. \tag{19b}$$

The plate has free edges and electrical open-circuited conditions at $y = 0$, $y = b$ as follows:

$$\sigma_y = \tau_{xy} = \tau_{zy} = D_y = 0, \tag{20}$$

where $\tau_{xy} = 0$, $\tau_{zy} = 0$, $D_y = 0$ are satisfied automatically. The remaining boundary condition to be satisfied is $\sigma_y = 0$. Due to symmetry, we only impose the condition at $y = 0$, and substitute the second equation of Eq. (9) into the first expression of Eq. (20) yields

$$\sum_{n=0}^{\infty}[\alpha_{13}\cdot\eta\cdot\bar{v}_n(z) + \alpha_{14}\cdot Z_n(z) + \alpha_{15}\cdot D_n(z)] + \alpha_{16}\cdot\varepsilon_0 - \alpha_{13}\cdot\frac{2}{b}\cdot v^{(0)}(z) = 0. \tag{21}$$

The following algebra equation system can be obtained by introducing Eqs. (18) and (19) and eventually the boundary unknown constants can be determined by considering Eqs. (21) and (22).

$$\begin{Bmatrix} v_n(z) \\ D_n(z) \\ Z_n(z) \end{Bmatrix} = -\begin{bmatrix} \Pi_{11}(z) & \Pi_{15}(z) & \Pi_{16}(z) \\ \Pi_{21}(z) & \Pi_{25}(z) & \Pi_{26}(z) \\ \Pi_{31}(z) & \Pi_{35}(z) & \Pi_{36}(z) \end{bmatrix} \begin{bmatrix} \Pi_{21} & \Pi_{25} & \Pi_{26} \\ \Pi_{31} & \Pi_{35} & \Pi_{36} \\ \Pi_{41} & \Pi_{45} & \Pi_{46} \end{bmatrix}^{-1} \begin{Bmatrix} \overline{\Pi}_2 \\ \overline{\Pi}_3 \\ \overline{\Pi}_4 \end{Bmatrix} + \begin{Bmatrix} \overline{\Pi}_1(z) \\ \overline{\Pi}_2(z) \\ \overline{\Pi}_3(z) \end{Bmatrix}. \tag{22}$$

## 3. Numerical examples and results

To validate the present method, numerical examples are presented for symmetric cross-ply piezoelectric laminated plates and comparisons are made between the current solution and work done by Artel and Becker [13], and Mirzababaee and Tahani [14]. The free-edge effect in the laminated plate with and without electromechanical coupling is investigated and two laminated layups $[0^\circ/90^\circ]_s$ and $[90^\circ/0^\circ]_s$ are considered. The material properties are given in Table 1 which comprises the mechanical properties of a T300/Epoxy and the piezoelectric and electrical properties of a PZT-5A. The uniaxial extension $\varepsilon_0$ is 0.1% and the width $b$ is ten times larger than the thickness $h$, in addition, the thickness of each ply in the laminate is identical.

Table 1. Mechanical and electrical properties of the piezoelectric plate

| Elastic Stiffness (GPa) | Piezoelectric Coefficients ($C/m^2$) | Dielectric Properties ($C^2/(Jm)$) |
|---|---|---|
| $C_{11}$=137<br>$C_{12}$=$C_{13}$=3.75<br>$C_{22}$=$C_{33}$=10.9<br>$C_{23}$=3<br>$C_{44}$=3.97<br>$C_{55}$=$C_{66}$=5 | $e_{31}$=$e_{32}$=-5.4<br>$e_{33}$=15.8<br>$e_{24}$=$e_{15}$=12.3 | $\epsilon_{11}$=$\epsilon_{22}$=1730$\epsilon_0$<br>$\epsilon_{33}$=1700$\epsilon_0$<br>$\epsilon_0$=8.859×$10^{-12}$ |

Distributions of stresses and electric field strength components at the $[0^o/90^o]$ interface in a $[0^o/90^o]_s$ laminate and at the $[90^o/0^o]$ interface in a $[90^o/0^o]_s$ laminate are presented for the electromechanical uncoupled and coupled cases. From Fig. 2 it is very clear that interlaminar normal stress $\sigma_z$ shows a possible singular behavior in the vicinity of free edge and ascends to a finite value at the free edge for both cases. For the coupled electric and mechanical circumstance, there is a good agreement between present results and those of Artel and Becker [13], and Mirzababaee and Tahani [14]. In addition, the values of coupled one are approximately two times larger than those of uncoupled one in the present results.

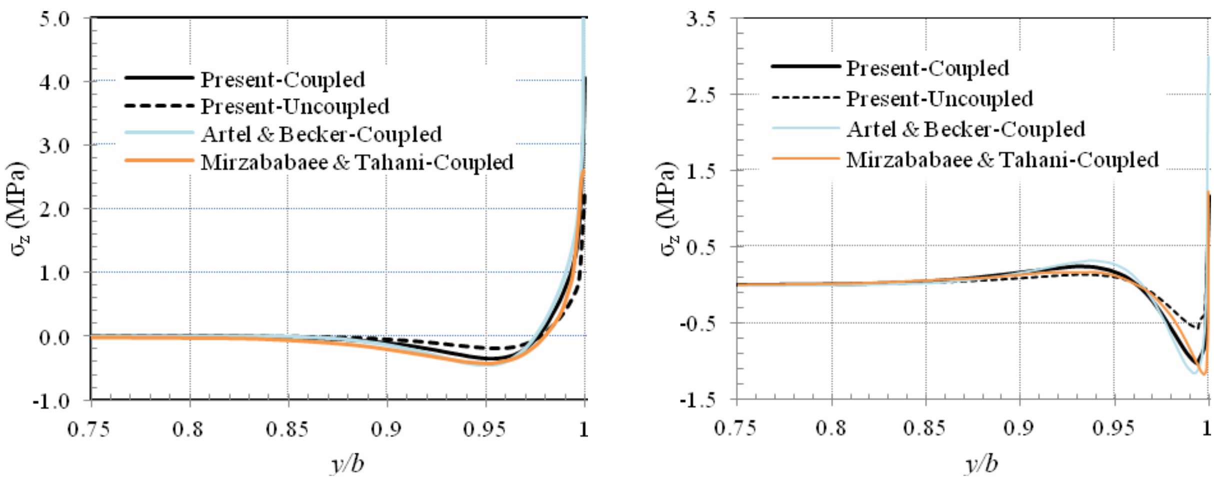


(a) $[0^o/90^o]_s$ (b) $[90^o/0^o]_s$

Figure 2. Distributions of interlaminar normal stress $\sigma_z$

The variations of interlaminar normal stress $\sigma_z$ at the interfaces through thickness at the free edges are depicted in Fig. 3. It is shown that the present uncoupled results have good agreement with those of Mirzababaee and Tahani [14] and the present coupled results have decent agreement with those of Mirzababaee and Tahani [14]. However, neither of above results for uncoupled and coupled is in good agreement with those of Artel and Becker [13], especially at the interfaces between different material plies. From Fig. 3 it is seen that the values of present coupled results are also approximately two times larger than those of present uncoupled results quantitatively.

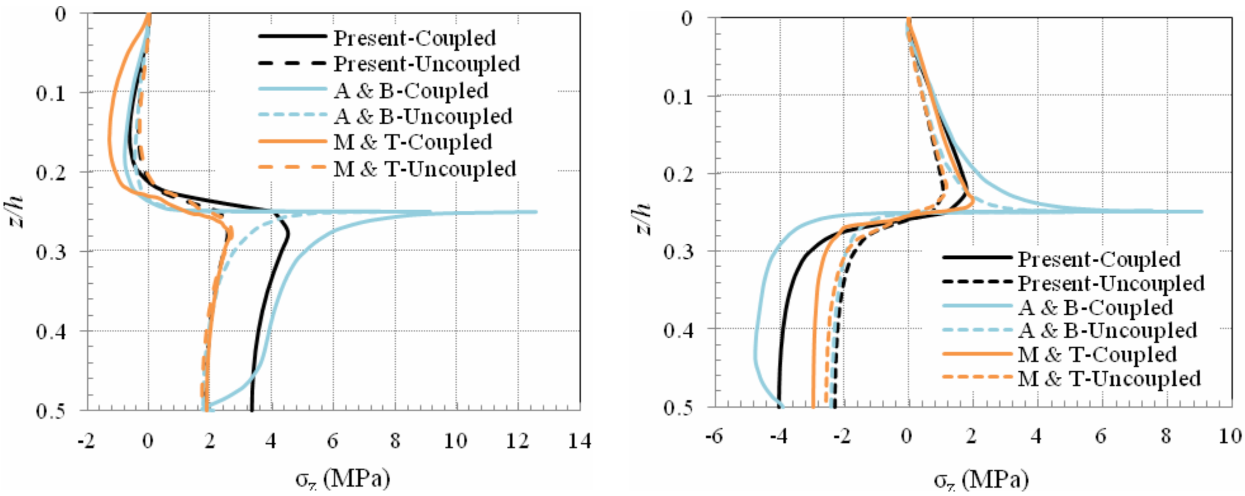


(a) $[0^o / 90^o]_s$ (b) $[90^o / 0^o]_s$

Figure 3. Through thickness variations of interlaminar normal stress $\sigma_z$

The variations of interlaminar stress $\tau_{yz}$ for uncoupled and coupled ones are shown in Fig. 4. The present results agree well with those of Artel and Becker [13], and Mirzababaee and Tahani [14] near the free edge. The value of $\tau_{yz}$ changes abruptly near the free edge at the interface and descends to zero at the free edge. In contrast to present results, those of Artel and Becker [13], and Mirzababaee and Tahani [14] cannot satisfy the traction free condition along free edges. Present results shows that interlaminar stress gradient occurs near the free edge due to the dissimilar properties of adjacent plies and coupled stresses are larger than those of uncoupled.

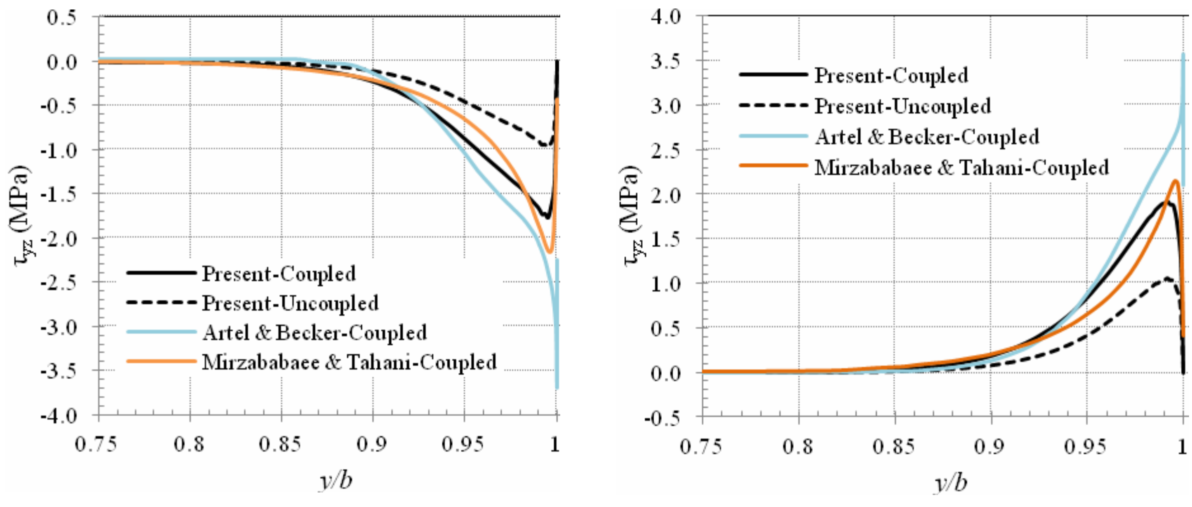


(a) $[0^o / 90^o]_s$ (b) $[90^o / 0^o]_s$

Figure 4. Distributions of interlaminar shear stress $\tau_{yz}$

Electrical quantities gradient may also occur in the vicinity of free edge at interfaces. The electric field component $E_y$ changes dramatically near the free edge and vanishes at the free edge. Moreover, another electric field component $E_z$ becomes singular at the free edge. In addition, it is worth to mention that present results disagreed with those of Artel and Becker [13], and Mirzababaee and Tahani [14] in magnitude.

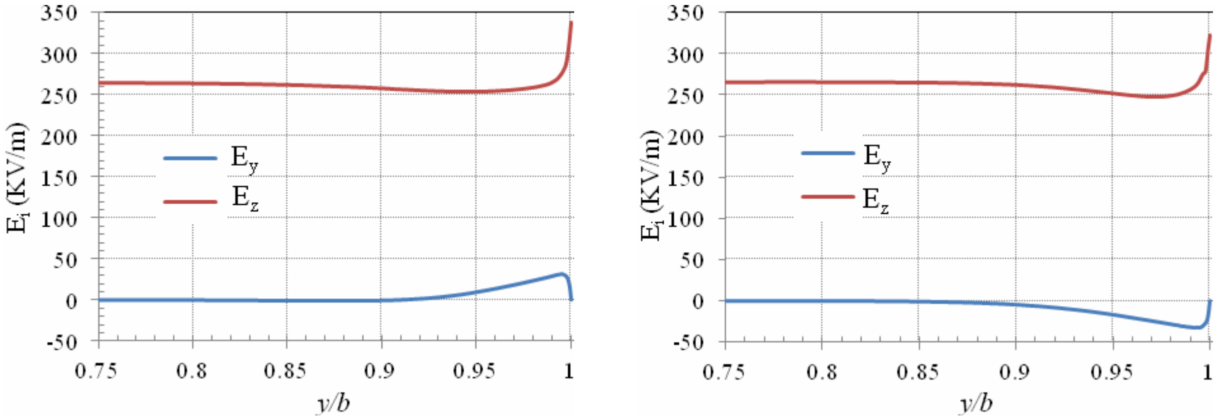


(a) $[0^o / 90^o]_s$ (b) $[90^o / 0^o]_s$

Figure 5. Distributions of electric field strength components $E_i$

On the basis of comparative analyses in this section, it is seen that the results of Artel and Becker [13], and Mirzababaee and Tahani [14] violate traction free boundary conditions at free edges. Furthermore, the FEM solution from Artel and Becker [13] fails to guarantee the continuity of transverse normal stress at interface of two different materials, deficiencies mentioned above were overcome by present solution. Both the stress and electric field strength singularities were observed with suitable layer refinement in *z*-direction.

## 4. Conclusions

State space method for an analytical solution has been developed to investigate the coupling effect on piezoelectric laminated plates and the singularities in the vicinity of free edges. Cross-ply laminated plates with and without electromechanical coupling subjected to uniform axial strain have been studied. To validate this method, comparisons were made between present results and those of other analytical and FEM solutions in the literature.

By satisfying all the mechanical and electric boundary conditions, especially tractions free conditions at free edges, and guaranteeing the continuity of transverse stresses and electric quantities across the interfaces between different material plies, the solutions show a significant piezoelectric effect on the laminated plate near the free edges and interlaminar stresses increase magnificently in coupled circumstance compared with those of uncoupled.

## References

[1] P. Heyliger, Exact solution for simply supported laminated piezoelectric plates. J. Appl. Mech. Trans. ASME. 64 (1997) 299-306.
[2] J.S. Lee, L.Z. Jiang, Exact electroelastic analysis of piezoelectric laminae via state space approach. Int J. Solids Struct. 33 (1996) 977-990.
[3] Z.Q. Cheng, C.W. Lim, S. Kitpornchai, Three-dimensional exact solution for inhomogeneous and laminated piezoelectric plates. Int. J. Eng. Sci. 37 (1999) 1425-1439.
[4] K. Xu, A.K. Noor, Three-dimensional analytical solution for coupled thermoelecroelastic response of multilayered plates. Comput. Methods Appl. Mech. Eng. 126 (1995) 355-371
[5] H.Y. Sheng, H. Wang, J.Q. Ye, State space solution for thick laminated piezoelectric plates with clamped and electric open-circuited boundary conditions. International Journal of Mechanical Sciences. 49 (2007) 806-818.
[6] R.B. Pieps, N.J. Pagano, Interlaminar stresses in composite laminates under uniform axial

extension. J. Compos. Mater. 4 (1970) 538-548.
[7] S.G. Lehknitskii, Theory of elasticity of anisotropic elastic body. Holden Day, San Francisco, 1963.
[8] S.S. Wang, I. Choi, Boundary-layer effects in composite laminates. Asme J Appl Mech. 49 (1982) 541-560.
[9] W. Becker, Closed-form solution for the free-edge effect in cross-ply laminates. Compos Struct. 26 (1993) 39-45.
[10] M. Tahani, A. Nosier, free edge analysis of general cross-ply composite laminates under extension and thermal loading. Compos Struct. 60 (2003) 91-103.
[11] D. Zhang, J.Q. Ye, H.Y. Sheng, Free-edge and ply cracking effect in cross-ply laminated composites under uniform extension and thermal loading. Compos Struct. 76 (2006) 314-325.
[12] R.Q. Ye, L.H. He, Electric field and stresses concentrations at the edge of parallel electrodes in piezoelectric ceramics. International journal of solids and structures. 38 (2001) 6941-6951.
[13] J. Artel, W. Becker, Coupled and uncoupled analysis of piezoelectric free-edge effect in laminated plates. Compos Struct. 69 (2005) 329-335.
[14] M. Mirzababaee, M. Tahani, Accurate determination of coupling effects on free edge interlaminar stresses in piezoelectric laminated plates. Materials and Design. 30 (2009) 2963-2974.